

Acidic and Catalytic Properties of the Ca-Pt-H-Mordenite System

SAVITA VISHNOI AND PAUL RATNASAMY¹

Indian Institute of Petroleum, Dehradun 248 005, India

Received March 2, 1981; revised June 23, 1981

The acid strength distribution and catalytic behavior (activity, selectivity, and deactivation in the reactions of *ortho*-xylene) of H-mordenite (HM), calcium mordenite (CaM), platinum H-mordenite (PtHM), calcium platinum H-mordenite (CaPtHM) and calcium platinum H-dealuminated-mordenite (DCaPtHM) have been studied. Measurement of the isosteric heats of adsorption of NH₃ indicate that the concentration of strong acid sites in these catalysts follow the order: HM > DCaPtHM > CaPtHM > PtHM > CaM. Their initial activity for the conversion of *ortho*-xylene decreases as HM > DCaPtHM > PtHM > CaPtHM > CaM. The selectivity of these catalysts in yielding isomeric xylenes rather than non-C₈ aromatics by disproportionation reaction decreases in the following order: CaM > DCaPtHM > HM > CaPtHM > PtHM. The catalyst undergo deactivation due to coke formation in the following order: HM ≫ DCaPtHM > CaPtHM > PtHM = CaM. An attempt is made to correlate the observed catalytic behavior with the acidic and steric features of the catalysts.

I. INTRODUCTION

The catalytic properties of mordenite-based catalysts have been studied quite extensively and there are even commercial processes for hydrocarbon conversion that utilize such catalysts (1). One major drawback in the use of mordenite as a catalyst is its fast deactivation, probably due to the deposition of carbonaceous material in its pores, during the process (2). H-Mordenite has a large pore dimension and being highly acidic, is very active for such acid-catalyzed reactions like the isomerization of xylenes and disproportionation of toluene. However, it is deactivated very fast in a few hours. Walsh and Rollmann have recently shown (3) that coke formation during the reactions of alkyl aromatics over zeolites is spatially demanding and depends mainly on the pore dimensions of the zeolite, less coke being formed over zeolites possessing 10 ring pores (like ZSM-5) than those with 12-ring pores (like mordenite and Y).

¹ To whom all correspondence should be addressed at: National Chemical Laboratory, Poona 411 008, India.

The main channel system in mordenite is one-dimensional in nature. When multivalent ions are present as the nonframework, exchangeable, cations in mordenite pores, they stick out from the channel walls and reduce the effective diameter of the pores. What is the influence of such pore size modulation on the catalytic activity, selectivity, and stability of mordenite in isomerization of xylenes? In addition to the steric factor, it is also possible that the selectivity behavior of mordenites can be modulated by the type and strength of their acid sites. What is the acid strength distribution of sites generated by the incorporation of ions like calcium or platinum? Even though the acidic and catalytic properties of dealuminated hydrogen mordenite, containing a lower density of acid sites, have been well studied (4), the consequences of lowering the effective pore dimension in such acidity-attenuated mordenite, by incorporation of ions like calcium, or/and platinum, on their catalytic behavior is still not clear.

In the present study, the acid strength distribution and catalytic behavior (activity, selectivity, and deactivation) of H-mor-

denite, calcium mordenite, platinum H-mordenite, calcium platinum H-mordenite and calcium platinum H-dealuminated mordenite in the isomerization of *o*-xylene have been studied. It is shown that by modulation of both the steric and acidic parameters it is feasible to prepare mordenite-based catalysts which have good activity, selectivity and stability.

II. EXPERIMENTAL

Materials

Sodium mordenite (NaM) and hydrogen mordenite (HM) in the form of $\frac{1}{8}$ -in.-size extrudates were procured from Norton Company (Zelon 100). Calcium mordenite (CAM) was prepared as follows: 30 g of NaM was continuously stirred in 1.0 M aqueous CaCl_2 for 5 hr in a beaker on a steam bath. Catalyst was then filtered and washed several times with distilled water. This exchange procedure was repeated six times. Catalyst was then dried at 383 K. Analysis of the filtrate by flame photometry indicated that the degree of exchange of sodium by calcium was 90%. Pt-H-Mordenite (PtHM) was prepared as follows: 35 g of HM was stirred for 144 hr with a magnetic stirrer in a solution of aqueous $\text{Pt}(\text{NH}_3)_4\text{Cl}_2$ (Alfa Products) (0.7033 g of $\text{Pt}(\text{NH}_3)_4\text{Cl}_2$ in 100 ml distilled water) in a beaker at room temperature. Catalyst was then washed with distilled water and activated at 773 K for 5 hr in a muffle furnace to decompose $\text{Pt}(\text{NH}_3)_4\text{Cl}_2$. By analysis the sample was found to contain 0.37wt% Pt. Calcium platinum hydrogen mordenite (CaPtHM) was prepared as follows: 10 g of PtHM was stirred in 0.1 M aqueous CaCl_2 for 5 hr in a beaker at room temperature. The catalyst was then washed with distilled water several times and dried at 383 K for 3 hr. The sample contained 0.24wt% Pt and 0.17wt% Ca. Dealuminated Ca-Pt-H-mordenite (DCaPtHM) was prepared as follows: Mordenite having a $\text{SiO}_2/\text{Al}_2\text{O}_3$ ratio of 14 was first prepared by using the method of Kerr (5) from NaM. The sample

was then exchanged with 0.1 M aqueous NH_4Cl at room temperature for 6 hr and filtered. The procedure was repeated until Na ions could not be detected in the filtrate. The catalyst was then heated at 773 K for 5 hours in a muffle furnace to decompose NH_4^+ ions yielding dealuminated H-mordenite. Platinum and calcium were next successively incorporated into this material, by procedures illustrated earlier, yielding DCaPtHM. The physicochemical properties of the catalysts are summarized in Table 1.

Ammonia gas (>99.9%) was obtained from Air Products. *Ortho*-xylene (Merck) was passed through activated silica gel and distilled before use.

Procedures

X-Ray diffractograms of the samples were taken using a GE XRD6 Diffractometer using $\text{CuK}\alpha$ radiation. The adsorption isotherms of ammonia were measured volumetrically using a conventional, high-vacuum adsorption system. Before the adsorption measurements, the samples (0.5 g) were degassed at 773 K for 6 hr under a vacuum of 10^{-5} Torr. They were then cooled to the isotherm temperature and the adsorption isotherm was measured. A fresh batch of sample was used for each isotherm run. Duplicate runs were carried out in most cases to establish reproducibility of the results. The chemisorption of NH_3 in the temperature range 513–573 K on these samples was found to be reversible as most of the adsorbed NH_3 molecules could be desorbed on prolonged evacuation at slightly higher temperatures.

The reactions of *o*-xylene on these catalysts were studied at atmospheric pressure in a down-flow, fixed-bed reactor. About 1 g of catalyst particles (16–20 mesh) were diluted with quartz chips of the same size in the ratio 1 : 1. Experiments were carried out in the temperature range 623–773 K and $\text{LHSV} = 1.4$. The products were analyzed by a gas chromatograph (Toshniwal) using a flame ionization detector and a (4 m \times 3

mm) column packed with 5% diisodecyl phthalate and 5% bentone-34 on chromosorb C. The column temperature was 90°C (isothermal). Hydrogen was used as the carrier gas (30 ml/min).

The chemical composition of the various catalyst samples was determined by conventional methods of wet analysis. Their surface areas were determined by the BET method using nitrogen at liquid nitrogen temperature. The platinum surface areas in PtHM, CaPtHM, and DCaPtHM were determined by titration of oxygen with preadsorbed H₂ on the Pt metal using the method of Benson and Boudart (6).

III. RESULTS

1. Composition and Structure

The chemical composition, surface area and Pt dispersion of all the catalysts of the present study are tabulated in Table 1. There is a slight reduction in surface area when NaM is converted to CaM (298–250 m²/g) or when PtHM is converted to CaPtHM (451–420 m²/g), which may be due to the partial blocking of the microchannels

of mordenite by the larger cation, Ca²⁺. Another point to be noted is the decrease in the Na content in the series HM > PtHM > CaPtHM > DCaPtHM (0.75, 0.36, 0.27 and 0.20 wt%, respectively). Apparently, during the incorporation of Pt²⁺ or Ca²⁺ in the mordenite, part of the Na ions are exchanged for the divalent Pt or Ca ions.

The X-ray diffractograms of the samples are shown in Fig. 1. In agreement with earlier investigations (7–10) neither acid extraction nor ion exchange caused any marked shift in the line positions.

2. Surface Acidity

Adsorption isotherms of NH₃ on all the samples were measured at different temperatures in the range of 510–573 K. The isotherm data were fitted successively to the adsorption isotherm equations of Langmuir, Freundlich, and Temkin by the method of least squares using a computer. The linear correlation coefficient *R* (11) was calculated for each set of data. In all cases, the Langmuir equation was found to fit the data most consistently and accurately, the values of *R* in all cases being above 0.98.

TABLE I
Physicochemical Properties of Catalysts

| | Catalyst | | | | | |
|----------------------------------|----------|-------|-------|-------|--------|---------|
| | NaM | CaM | HM | PtHM | CaPtHM | DCaPtHM |
| WT. % | | | | | | |
| Loss on ignition (wt%) | 5.04 | 4.83 | 10.11 | 10.13 | 10.91 | 12.68 |
| Component (wt%) | | | | | | |
| SiO ₂ | 75.8 | 75.8 | 77.05 | 77.65 | 76.05 | 76.44 |
| Al ₂ O ₃ | 12.24 | 12.24 | 11.05 | 11.5 | 11.5 | 9.4 |
| Fe ₂ O ₃ | 0.72 | 0.72 | 0.59 | 0.59 | 0.59 | 0.55 |
| Na ₂ O | 6.26 | 0.62 | 0.75 | 0.36 | 0.27 | 0.20 |
| CaO | — | 5.79 | — | — | 0.24 | 0.14 |
| Pt | — | — | — | 0.37 | 0.24 | 0.29 |
| Surface area (m ² /g) | 298 | 250 | 457 | 451 | 420 | 439 |
| Pt dispersion (%) | — | — | — | 50 | 72.5 | 31.5 |

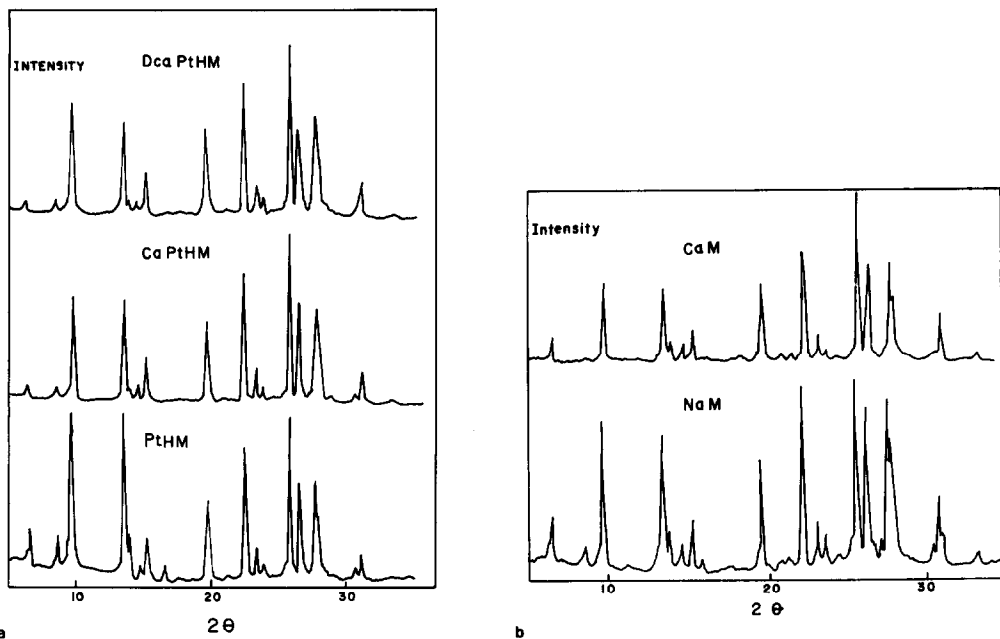


FIG. 1. (a) X-Ray diffractograms of PtHM, CaPtHM, and DCaPtHM. (b) X-Ray diffractograms of NaM and CaM.

In order to obtain the acid strength distribution of the sites adsorbing ammonia, the isosteric heat of adsorption, q_{st} was calculated at various coverages in the range 0.5–1.5 of θ , the millimoles of NH_3 (NTP) adsorbed per gram of solid, using the integrated form of the Clausius-Clapeyron equation. The variation of q_{st} with θ for NaM, HM, CaM, PtHM, CaPtHM, and DCaPtHM is shown in Fig. 2. The heat of liquifaction of NH_3 is 5.58 kcal/mol. Since all the values of q_{st} upto a monolayer coverage on all the samples studied are significantly higher than the above value, it is concluded that NH_3 is strongly chemisorbed on these samples under our experimental conditions. The total theoretical acidity for mordenite (one molecule of NH_3 per Al ion) is about 2.61 mmol/g of zeolite. Hence, all the data presented in Fig. 2 refer to the submonolayer region. The change in q_{st} for HM with coverage is quite similar to that reported by Kiovsky *et al.* (12) for a similar sample. Values of q_{st} and their variation with coverage for the other samples

have not been reported in the literature so far.

Following Clark *et al.* (13), the differential molar entropies of adsorbed NH_3 molecules, \bar{S}_Γ , were calculated from the following equations:

$$-\Delta\mu_\Gamma = RT \ln P_\Gamma, \quad (1)$$

$$-\Delta\bar{S}_\Gamma = \frac{\Delta\mu_\Gamma + q_{st}}{T}, \quad (2)$$

$$\bar{S}_\Gamma = S_G + \Delta\bar{S}_\Gamma, \quad (3)$$

where

P_Γ = the equilibrium pressure of NH_3 at a surface concentration, Γ ;

$\Delta\mu_\Gamma$ = the partial molar free energy of adsorption;

$\Delta\bar{S}_\Gamma$ = the differential molar entropy of adsorption relative to the standard state of gaseous NH_3 at 1 atm;

S_G = molar entropy of gaseous NH_3 at 1 atm;

and

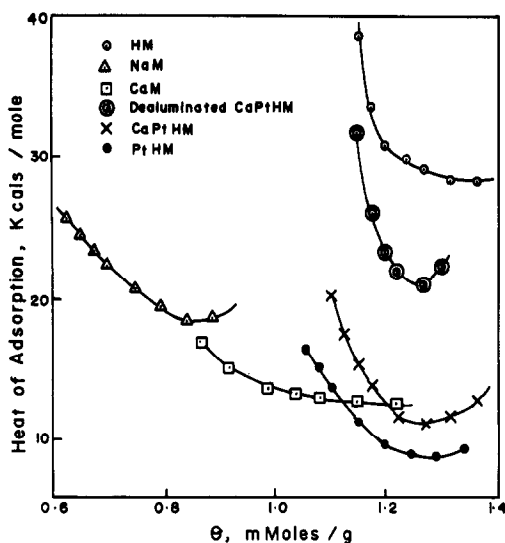


FIG. 2. Variation of the isosteric heat of adsorption, q_{st} , with coverage.

\bar{S}_T = the differential molar entropy of adsorbed NH_3 molecules.

The values of \bar{S}_T for NH_3 adsorbed on our samples are shown in Figs. 3–5. The entropies of gaseous NH_3 at 240, 270 and 300° are 51.0, 51.75, and 52.3, e.u., respectively (14).

The heat of adsorption decreases with coverage for all the samples (Fig. 2). At higher coverages there is a slight increase in q_{st} arising, probably, from the interaction between adsorbed NH_3 molecules. The strongest acid sites occur on HM ($q_{st} > 30$ kcal), while in the case of NaM and CaM, q_{st} remains low even at low coverages of adsorbed NH_3 . When platinum or platinum plus calcium are incorporated into the HM zeolite the heat of adsorption of NH_3 is drastically suppressed (Fig. 2).

This phenomenon is also reflected in the higher entropy of NH_3 molecules adsorbed on PtHM and CaPtHM compared to those on HM (Figs. 3 and 5). The entropy of adsorbed molecules is directly related to their mobility and the degree of freedom for vibration and rotation possessed by them in the adsorbed state. Strong acid site–basic molecule interactions lead to high heats of

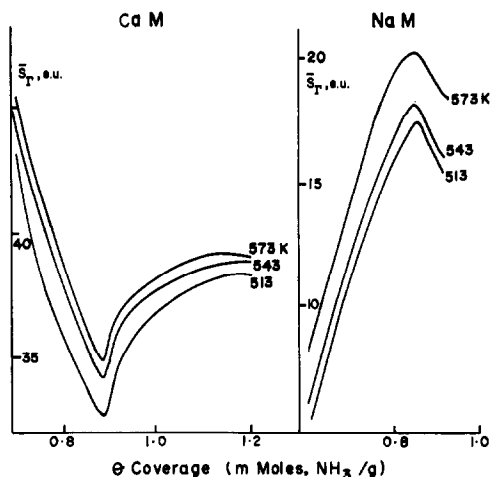


FIG. 3. Variation of \bar{S}_T , the differential molar entropy of adsorbed ammonia, with coverage for CaM and NaM.

adsorption and low mobility of the adsorbed basic molecules. At similar values of surface coverage, the entropy of adsorbed NH_3 molecules decrease in the order PtHM > CaPtHM > HM. When platinum plus calcium are incorporated in dealuminated HM (as in DCaPtHM), however, the heat of adsorption of NH_3 is significantly higher (Fig. 2) and the entropy of adsorbed NH_3 is correspondingly low-

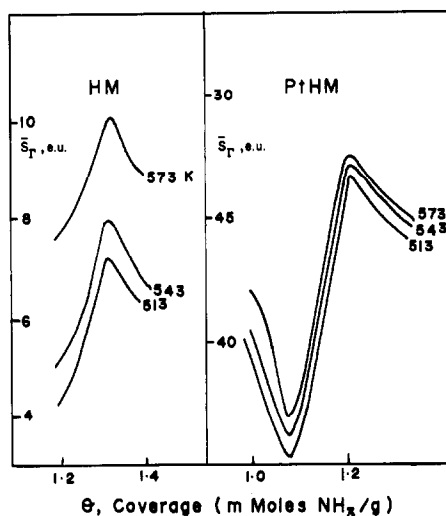


FIG. 4. Variation of \bar{S}_T , the differential molar entropy of adsorbed ammonia, with coverage for HM and PtHM.

ered. Now, during dealumination, Al^{3+} ions are removed from the lattice framework and since the acid sites in mordenite are linked to the presence of these Al^{3+} ions, their removal will lead to lower acid site densities and lower concentration of adsorbed NH_3 molecules in DCaPtHM. One consequence of this will be that observed heats of adsorption of NH_3 will increase since repulsive interactions among adsorbed NH_3 molecules will now be attenuated.

3. Catalytic Activity

The reactions of *o*-xylene over acidic catalysts may be represented by the following reaction sequence (17)



In addition, disproportionation (yielding toluene and trimethylbenzene) and dealkylation (yielding toluene and further, benzene) reactions can, also, occur. Three parameters were used to characterize the catalytic activity, isomerization efficiency, and stability, respectively.

(1) The activity of the catalyst was char-

acterized by an apparent first order rate constant, k , where

$$k = \frac{1}{W} \ln \frac{1}{1-x} \quad (5)$$

In the above equation,

W = the weight of the catalyst in grams and
 x = fractional conversion.

(2) The isomerization efficiency of the catalyst in yielding *para*- and *meta*-xylenes is defined in the following way:

$$\text{Isomerisation efficiency} = \frac{A}{B-C}$$

where

A = the sum of *para*- and *meta*-xylenes in product (wt%),

B = *o*-xylene in feed (wt%),

C = *o*-xylene in product (wt%).

(3) Since all the catalysts were found to undergo deactivation with time, an attempt was made to describe the rate of deactivation, at least, semiquantitatively. The values of k derived from Eq. (5) above were fitted using a computer by multiple-regres-

TABLE 2
Catalytic Activity for *o*-Xylene Isomerization^a

| | Catalyst | | | | |
|--------------------------------|----------|------|-------|--------|---------|
| | HM | PtHM | CaM | CaPtHM | DCaPtHM |
| Temp. (K) | 673 | 623 | 673 | 673 | 673 |
| Rate const., k (g^{-1}) | 0.28 | 0.53 | 0.006 | 0.32 | 0.36 |
| Isom. efficiency | 0.85 | 0.60 | 1.0 | 0.80 | 0.95 |
| Prod. Comp. (wt.%) | | | | | |
| Benzene | 0.3 | 1.7 | — | 0.2 | 0.2 |
| Toluene | 4.8 | 19.6 | — | 6.00 | 2.0 |
| <i>p</i> -Xylene | 13.2 | 10.2 | — | 12.6 | 20.3 |
| <i>m</i> -Xylene | 36.4 | 38.7 | 1.2 | 39.9 | 39.5 |
| <i>o</i> -Xylene | 41.8 | 18.7 | 98.4 | 34.3 | 37.1 |
| 1,3,5 TMB | — | 2.5 | — | 1.1 | — |
| 1,2,4 TMB | 3.6 | 8.7 | — | 5.1 | 0.9 |
| 1,2,3 TMB | — | — | — | 0.7 | — |
| E^* (kcal/mole) ^b | 15.8 | 20.5 | 15.8 | 17.1 | 17.8 |

^a LHSV = 1.0; H_2/o -xylene = 10.0; Pressure = atmospheric; time on stream = 4 h.

^b The apparent activation energy values E^* were determined from Arrhenius plots of the rate constants in the temperature range 623–673 K.

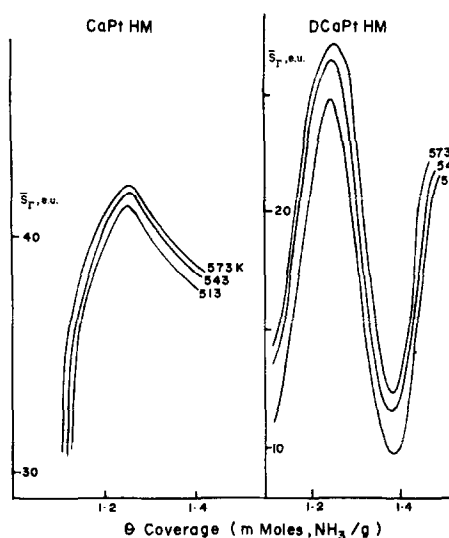


FIG. 5. Variation of \bar{S}_p , the differential molar entropy of adsorbed ammonia, with coverage for CaPtHM and DCaPtHM.

sion methods to the following equation:

$$k = k_0 e^{-\alpha Y}, \quad (6)$$

where Y is the cumulative amount of *o*-xylene that has been converted to products and k_0 and α are constants which characterize the initial activity and the aging rate of the catalyst, respectively.

The catalytic activity of the various catalysts for the isomerization of *o*-xylene are compared in Table 2. NaM possessed negligible activity for this reaction. The catalyst deactivation parameters, computed by fitting experimental data to Eq. (6) are given in Table 3. The aging behavior of the catalysts is illustrated in Fig. 6 for CaPtHM. The following conclusions may

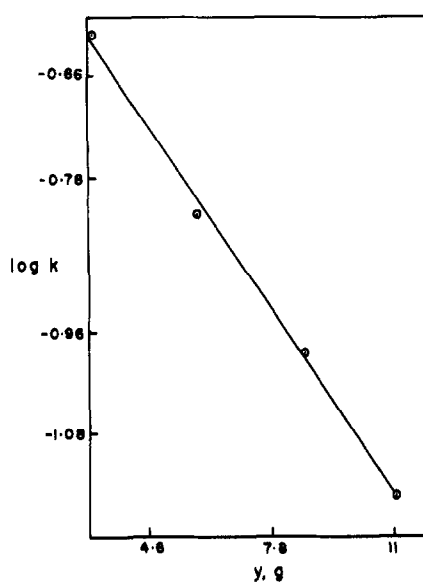


FIG. 6. Exponential catalytic deactivation for CaPtHM. Fit of experimental data (circles) to the model. The straight line was obtained from Eq. (6).

be drawn from the data: (1) Calcium mordenite (CaM) has negligible activity for *o*-xylene isomerization ($k = 0.006$). (2) The value of k , the rate constant, is higher for PtHM than for HM (0.53 vs 0.28). The isomerization efficiency, however, is lower for PtHM (0.60 vs 0.85 for HM) due mainly to the production of a large quantity of toluene and trimethylbenzenes by the disproportionation of *o*-xylene. PtHM catalysts, moreover, deactivate at a lower rate than HM ($\alpha = 0.03$ for PtHM and 0.14 for HM (Table 3)). (3) The activity, selectivity and stability of CaPtHM is intermediate between that of HM and PtHM (compare the

TABLE 3

Catalyst Deactivation Parameters in the Isomerization of *o*-Xylene^a

| | Catalyst | | | | |
|--|----------|------|-------|--------|---------|
| | HM | PtHM | CaM | CaPtHM | DCaPtHM |
| Temp. (K) | 673 | 623 | 673 | 673 | 673 |
| Initial activity, k_0 (g ⁻¹) | 1.25 | 0.80 | 0.015 | 0.66 | 0.93 |
| "Aging" constant, α | 0.14 | 0.03 | 0.03 | 0.07 | 0.10 |

^a H₂/*o*-xylene = 10; LHSV = 1; pressure = atmospheric.

values of k , isomerization efficiency, and α). (4) DCaPtHM has good activity, excellent selectivity and good stability. It produces the maximum amount of *p*-xylene (20.3%), while producing very small amounts of trimethylbenzenes and toluene. (5) Among the three isomers of trimethylbenzenes, the 1, 2, 4 isomer, possessing the minimum cross section (7.6 Å vs 8.1 and 8.6 Å for the 1, 2, 3 and 1, 3, 5 isomers, respectively), was the predominant product at all conversion levels over all the mordenite based catalysts investigated even though the 1, 3, 5 isomer is the thermodynamically favored one. In fact, over HM, up to a conversion level of *o*-xylene of 50% both the 1, 3, 5 and 1, 2, 3 isomers were absent (Fig. 7). Similar shape-selective disproportionation of xylenes was also reported by Yashima *et al.* (18).

IV. DISCUSSION

The salient points of the present study may be summarized as follows: (1) The total number of acid sites is lower when the nonframework cations in mordenite are calcium, platinum, or calcium and platinum, rather than protons. (2) The initial activity of the catalysts (Table 3) for the conversion of *o*-xylene falls in the following order: HM

> DCaPtHM > PtHM > CaPtHM > CaM > NaM. (3) The selectivity (isomerisation efficiency) of the catalysts (Table 2) are: CaM > DCaPtHM > HM > CaPtHM > PtHM. (4) The catalysts undergo deactivation (Table 3) in the following order: HM \gg DCaPtHM > CaPtHM > PtHM = CaM.

(a) Activity

The conversion of *o*-xylene to various products is an acid-catalyzed process. It is, hence, not surprising that the initial activity of the catalysts (Table 3) is proportional to their surface acidity. HM, possessing sites of highest acid strength, is also the most active catalyst, followed by DCaPtHM. The least active among the catalysts NaM, is also the least acidic as judged from q_{st} values at low coverages of adsorbed NH_3 molecules (Fig. 2). The lower catalytic activity of CaPtHM compared to PtHM, even though its acidic sites are stronger than those of the latter is probably due to the presence of calcium ions in the zeolite pores. While they may not sterically inhibit the adsorption and diffusion of the small NH_3 molecule (cross section = 2.6 Å), they may have a retarding effect on the movement of *o*-xylene (cross section = 7.6 Å). In the case of DCaPtHM, however, due to the lower concentration of the total nonframework cations (Table 1), the magnitude of such steric inhibition is lower ($k = 0.36$ vs 0.32 g^{-1} for CaPtHM).

(b) Selectivity

In the presence of acid catalysts, in addition to isomerising to a mixture of *meta*- and *para*-xylenes, *ortho*-xylene also undergoes disproportionation to yield toluene and trimethylbenzenes. Dealkylation reactions (xylene \rightarrow toluene \rightarrow benzene) may also occur. Even though all the above reactions are catalyzed by acid sites, additional parameters like the density of acid sites and pore dimension will also influence the selectivity of a catalyst to undergo disproportionation.

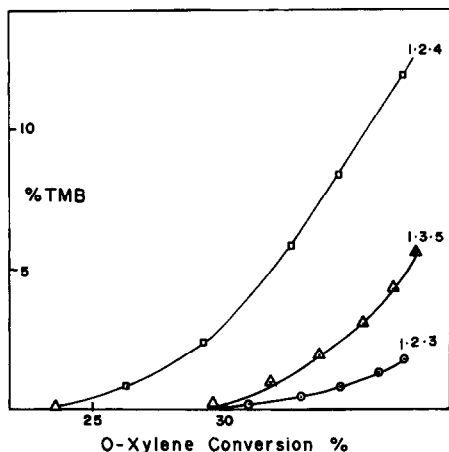


FIG. 7. Shape selectivity: concentration of various trimethylbenzene isomers as a function of *o*-xylene conversion.

tionation reactions. Since the disproportionation reaction involves the reaction of two xylene molecules adsorbed on adjacent acid sites, higher acid site densities will lead to higher concentrations of trimethylbenzenes in the product. Similarly, since a diphenylmethane type intermediate is probably involved in the formation of trimethylbenzene (19), larger concentrations of trimethylbenzenes may be expected over catalysts with wider pores, other factors remaining the same. Now, applying the above concepts to the product distribution data in Table 2, we observe that the isomerization efficiency (which measures the selectivity for isomerisation to C₈ aromatics) is high in the case of CaM and DCaPtHM, both of which have low acid site densities and low effective pore diameters. Even though HM, PtHM and CaPtHM have high activity, their isomerization efficiency is low, due to the relatively higher density of acid sites on them.

(c) Stability

All the catalysts used in the present study underwent deactivation during the reaction (Table 3). Their activity could be restored to the initial level by oxidation procedures involving the burning-off the deposited carbon. Catalytic deactivation did not bring about any structural changes as could be seen from the X-ray diffraction spectra of regenerated samples. Their adsorption behavior (for adsorption of benzene) was also similar to those of the fresh samples. It may, hence, be concluded that the main cause of deactivation was the deposition of coke in the pores of the zeolites. From the data in Table 3, it is difficult to draw any simple correlation between the "aging" constant, α , and any one of the physicochemical characteristics of the catalyst. Samples like HM having strongly acidic sites (as judged by the heats of adsorption of NH₃ (Fig. 2)) undergo fast deactivation and those like PtHM and CaM with weak acid sites have lower values of α .

V. CONCLUSION

It is feasible to prepare a mordenite-based catalyst for the isomerization of xylenes which was high isomerization activity, low selectivity for the formation of non-C₈ aromatics and good stability against deactivation by coke deposition. Dealuminated calcium platinum hydrogen mordenite (DCaPtHM) possessing a lower density of acidic sites (than HM) and containing calcium and platinum ions in the zeolitic pores has been found to be an excellent catalyst for the isomerization of *o*-xylene to an isomer mixture of near equilibrium composition.

ACKNOWLEDGMENT

S. V. thanks the Council of Scientific and Industrial Research for a fellowship.

REFERENCES

1. Jacobs, P. A., "Carboniogenic Activity of Zeolites," Elsevier, Amsterdam, 1977.
2. Burnbridge, B. W., Keen, I. M., and Eyles, M. K., "Advances in Chemistry," Vol. 102, p. 400, Amer. Chem. Soc., Washington, D.C., 1971.
3. Walsh, D. E., and Rollman, L. D., *J. Catal.* **56**, 195 (1979).
4. Miradatos, C., Ha, B. H., Otsuka, K., and Barthomeuf, D., in "Proceedings, 5th Intl. Conf. Zeolites," p. 382, Heyden, Philadelphia, 1980.
5. Kerr, G. T., *J. Phys. Chem.* **72**, 2594 (1968).
6. Benson, J. E., and Boudart, M., *J. Catal.* **4**, 704 (1965).
7. Eberly, P. E. and Kimberlin, C. N., *Ind. Eng. Chem. Prod. Res. Develop.* **9**, 335 (1970).
8. Belekaya, I. M., Dubinin, M. M., and Krishtofri, T. I., *Chem. Abstr.* **68**, 43515t (1967).
9. Dubinin, M. M., Fedorova, G. M., Plavink, G. M., Piguzova, L. P., and Prokofeva, E. N., *Chem. Abstr.* **70**, 41637c (1968).
10. Noriaki, N., Kishimura, Y., and Takashashi, H., *Bull. Japan Petrol. Inst.* **13**, 205 (1971).
11. Young, H. D., "Statistical Treatment of Experimental Data," p. 130. McGraw-Hill, New York, 1962.
12. Kiovsky, J. R., Goyette, W. J., and Noterman, T. M., *J. Catal.* **52**, 25 (1978).
13. Clark, A., Holm, V. C. F., and Blackburn, D. M., *J. Catal.* **1**, 244 (1962).

14. Kobe, K. A., and Harrison, R. H., *Petrol. Refiner*, **33**, 161 (1954).
15. Clark, A., and Holm, V. C. F., *J. Catal.* **2**, 21 (1963).
16. Breck, D. W., and Skeels, G. W., in "Proceedings 6th Intl. Congr. Catal., London, 1976," B4.
17. Cortes, A., and Corma, A., *J. Catal.* **51**, 338 (1978).
18. Yashima, T., Iwase, O., and Hara, N., *Chem. Lett. (Japan)*, 1215 (1975).
19. Csicsery, S. M., *J. Catal.* **19**, 394 (1970).